Open Ceramics 9 (2022) 100227

Contents lists available at ScienceDirect

Open Ceramics

journal homepage: www.sciencedirect.com/journal/open-ceramics

Effect of boron sources in the thermal behavior of a clay-based ceramics

María F. Hernández [a,b,*], Paula V. López [a,b], María S. Conconi [a,b], Nicolás M. Rendtorff [a,b]

[a] Centro de Tecnología de Recursos Minerales y Cerámica CETMIC (UNLP-CIC-CONICET) Cno, Centenario y 506 Gonnet, La Plata, 1897, Argentina
[b] Departamento de Química, Facultad de Ciencias Exactas UNLP, 47 y 115, La Plata, 1900, Argentina

ARTICLE INFO

Keywords:
Clay based ceramic
Dry processing
Boron sources
Processing and properties

ABSTRACT

Boron oxide sources as fluxing agents for clay-based materials have been a problem for the high solubility of these additives, however the dry milling-mixing-granulating route for clay based ceramics has been proposed and implemented with noticeable energetic advances.

In the present study, the role of different boron oxide sources in the thermal behavior and sinterability of ceramic materials based on kaolinite clay was evaluated.

Four boron sources were evaluated: Boric acid, borax, colemanite and ulexite. Four binary mixtures were made in a planetary mill to obtain uniform mixtures. For systematic comparison, the boron content added in all samples was 1 wt%. The thermal behavior evaluation of the mixtures was carried out by a multi-technique approach accompanied by textural, microstructural characterization complemented by a deep crystalline and non-crystalline phase evolution.

Ulexite and borax presented the highest fluxing effect and colemanite has an even more moderate effect than boric acid. The observed microstructure was similar to other clay-based ceramics, with quartz grains, cristobalite and mullite embedded in the silica-based vitreous phase.

The present study provides information for the additional design of clay-based materials with boron oxides as fluxing agents. The dry route alternative for using these agents was effective.

1. Introduction

Ceramics have been processed by different routes for millennia; wet (colloidal), plastic, semi dry and dry processing routes can be found in clay based ceramics. In the 20th century when the basic concepts of ceramic processing were established, it was demonstrated the important relationships that exist between the structure, properties and process variables [1–3].

Generally, the granulometric adaptation together with the mixing of formulations based on clay, quartz and fluxes is carried out in ball mills, in aqueous dispersions. Then, these dispersions are dried to achieve the proper water content for the forming route. Either for slips for casting on a completely liquid route or dehydrated (in filter presses) to a plastic state to shape by extruded or shaping on automatic wheels, for the manufacture of semi-dry granules, by spray drying, which is the classic consistency for uniaxial pressing of flat pieces. Spray drying consumes a considerable amount of energy [4,5].

Kaolinitic clays are used in a wide variety of industrial applications such as ceramics, refractories, cement, fillers in paper, plastics, rubber and cosmetics to achieve the desired properties. Heat treatments are involved in most of these applications [6,7].

Especially for tile, tableware and sanitary ware industries kaolinitic clays (kaolins) are the main or one of the main raw materials.

The most abundant phase of kaolinitic clays is kaolinite $Al_2O_3.2SiO_2.2H_2O\ (K)$, whose thermal transformations are affected by the selected heating program, particle size of the powders, impurities and sintering additives. The thermal transformations of kaolinite and quartz $SiO_2(Q)$, which generally accompanies the kaolinite, are detailed in the following equations [8].

$$Al_2O_3.2SiO_2.2H_2O\ (K) \rightarrow Al_2O_3.2SiO_2(MK) + 2H_2O \quad (1)$$

$$Al_2O_3.2SiO_2(MK) + SiO_2(Q) \rightarrow spinel\ Al-Si\ (SAS) + SiO_2(V) + SiO_2(Q) \quad (2)$$

$$Al_2O_3.2SiO_2(MK) + SiO_2(Q) \rightarrow 3Al_2O_3.2SiO_2(Mi) + SiO_2(V) + SiO_2(Q) \quad (3)$$

* Corresponding author. Centro de Tecnología de Recursos Minerales y Cerámica CETMIC (UNLP-CIC-CONICET) Cno, Centenario y 506 Gonnet, La Plata, 1897, Argentina.
E-mail address: florenciahernandez@cetmic.unlp.edu.ar (M.F. Hernández).

https://doi.org/10.1016/j.oceram.2022.100227
Received 23 December 2021; Received in revised form 25 January 2022; Accepted 27 January 2022
Available online 29 January 2022

$$spinel\ Al-Si\ (SAS)+SiO_2(V)\ \rightarrow 3Al_2O_3.2SiO_2(Mii)+\ SiO_2(V) \quad (4)$$

$$SiO_2(Q)\rightarrow SiO_2(C) \quad (5)$$

Sintering additives play a determining role in the ceramic process. Fluxing agents play a fundamental role in clay formulations, due to the need to obtain low levels of porosity in the resulting material. Low porosity is achieved by the formation of important volumes of liquid (or vitrous) phase during sintering, which is the result of the progressive melting of the flux minerals used in the ceramic composition. This process is sometimes accompanied with the formation of new crystalline phases, which can be formed within the vitreous magma [9]. Therefore, fluxing agents are decisive when defining the sintering temperature of the ceramic material [10]. This also leads to a direct decrease in energy consumption reducing energy costs.

The energy consumption in clay based ceramic industries is important and many times defines the viability of a determined production. In the most common wet ceramic route both the drying and firing are the most energy consuming operations. Porcelain stoneware tiles have traditionally been produced by the wet route [11,12]. However, growing concerns for the sustainability of ceramic tile production have opened the way for a new, dry processing route involving lower water and energy consumption and hence environmental benefits [13].

One of the main reasons that lead to this development is the fact that the dry route uses approximately 30% less thermal energy than the traditional wet route [13]. Among the different types of processing, production via the dry route has been proposed. In this, the milling-mixing operations and the subsequent granulation are carried out in dry (or quasi dry) conditions [14]. The wet routes require water-insoluble raw materials (initial powders) and complex rheological studies given the established formulations and operations. This is not the case of the dry route, where non plastic clays or very plastic clays can be employed. The sintering additives a mineralizer selection possibility is also broader in the dry route due to the incorporation of the soluble raw materials.

Borates can be interesting alternatives to use in ceramics, since B_2O_3 allows the formation of glassy phases with reduced viscosity at low temperature and is a glass network former [15]. These sintering additives have great potential for use in refractories to improve their thermo-mechanical properties at intermediate temperatures (600–1200 °C) [16,17]. Boron-based compounds are noted as suitable options for this purpose as they undergo phase transformations (decomposition, oxidation, etc.) at relatively low temperatures, which can lead to the generation of boron-rich liquid phase and transient sintering in liquid phase [18].

In recent studies, boron minerals have been incorporated into different ceramic compositions. Wastes from boron mineral refining have been incorporated into a sanitary clay based formulation, these wastes contain B_2O_3 and alkali oxides [15,19,20]. Waste from borax and colemanite refinements have been proposed as well. In total or partial replacement of feldspars [15,20] both agree that it is advantageous for the ceramic industry due to its reduction in sintering temperature and the low cost of raw material.

Furthermore, B_2O_3 has demonstrated to be a useful flux for sintering steatite powders of the MgO - Al_2O_3 - SiO_2 - BaO system. Highly dense and crystalline ceramics were obtained, together with small amounts of residual glass phase after sintering at low temperature (1200 °C). The viscous flow of B_2O_3 promoted the elimination of pores and increased densification, the flexural strength of ceramics increased with the content of B_2O_3 [21].

In a recent study ceramic materials have been made using a dry scalable process from binary mixtures of clay and boric acid (H_3BO_3) [22] and it is the main background to this article. In it, a systematic study of the effect of B_2O_3, incorporated as boric acid, in the thermochemistry of a kaolinite industrial clay was carried out, addressing through a multi-technical strategy based on various thermal analyzes, accompanied by determination of the crystalline and non-crystalline phases and the evaluation of the texture and developed microstructure. It was possible to describe the thermochemistry of the complex system and it was found that ceramics processed with 5% of B_2O_3 present rehydration problems.

The objective of this article is to study the effect of different boron sources in thermochemical processes and the ceramic behavior of industrial kaolinitic clay, in order to study the effect of the alkali/alkaline earth oxide that accompanies the boron. In particular, borax (B), colemanite (C) and ulexite (U), were studied and compared with boric acid (A) in binary mixtures with clay and the non added clay (T). We evaluate the changes in the technological properties of the resulting ceramic, using differential thermal analysis (DTA), thermogravimetric analysis (TG), dilatometric analysis (TMA) and conventional X-ray powder diffraction (XRD) with Rietveld refinement. This will enlighten the design strategies of dry clay-based ceramics processing routes.

2. Materials and methods

2.1. Raw materials

Industrial kaolinitic ball clay from Santa Cruz (Tincar S, PG La Toma Argentina) was used as the starting material [23]. Commercial boric acid (Borax Argentina SA, Argentina) with 99.8% of H_3BO_3, (56.2% B_2O_3); borax ($Na_2B_4O_7.10H_2O$), colemanite ($Ca_2B_6O_{11}.5H_2O$) and ulexite ($NaCaB_5O_9.8H_2O$) were used as sintering aids.

The kaolinitic ball clay contains Al_2O_3 (27.55 wt%) and SiO_2 (61.82 wt%) as well as small amounts of: 0.76 wt% K_2O, 0.79 wt% Fe_2O_3, 0.39 wt% TiO_2.

2.2. Sample preparation of starting mixtures

The samples without sintering aid are labeled T, T – A; T – B; T – C and T – U. T stands for Tincar kaolinitic clay, Ac stands for boric acid, B stands for bórax, C stands for colemanite and U stands for ulexite. All the compositions with 1 wt% of elemental boron (B). This is why the percentage by weight of each additive is different; 5.71 wt% for boric acid; 8.82 wt% for borax; 6.34 wt% for colemanite and 7.50 wt% for ulexite.

Dry milling was employed for avoiding solubility problems of the aids. A planetary ball mill was employed (Fritsch Pulverisette premium line 7). Zirconia jars (85 ml) and milling elements (10 mm diameter) were employed. Both the pure industrial clay and the mixtures were subjected to equivalent mixing-milling pretreatments. Afterwards, disc shape samples were uniaxially pressed (10 mm diameter) up to 100 MPa. These were sintered in an electric furnace, with air atmosphere, with 5 °C min^{-1} heating rate and 30 min soaking, and maximum temperatures between 1100 and 1400 °C.

2.3. Fired sample characterizations

The thermal behavior of the mixtures was studied. Simultaneous thermogravimetric (TG) and differential thermal analysis (DTA) and the dilatometry (TMA) were performed up to 1400 °C. Both thermal analyses were carried out simultaneously at a 5 °C min^{-1} heating rate in air atmosphere (TG-DTA and TMA Rigaku Evo plus II, Japan).

After this analysis, samples were fired at the same heating rate (5 °C min^{-1}) with different maximum temperatures in the range of 1100–1400 °C and 30 min soaking in air atmosphere.

The crystalline phases of sintered samples were determined by X-ray diffraction (XRD) using CuKα radiation operating at 40 kV and 300 mA (Philips PW1710). The XRD patterns were analyzed with the program FullProf (version 4.90, July 2010), which is a multipurpose profile-fitting program [24,25], including Rietveld – Le Bail refinement to perform phase quantification [26,27].

Open porosity was determined by Archimedean immersion method in distilled water and the pore size distribution of sample heated at

1300 °C was measured by mercury intrusion porosimetry.

Finally, a scanning electron microscope (SEM) (JEOL, JCM- 6000) was employed to describe the developed microstructures.

3. Results and discussions

3.1. Thermal behavior

A multi-technique approach was carried out for understanding the effect of the boron oxide and accessories oxides that accompany each of the boron sources studied in the thermochemical processes of the kaolinitic clay. From each analysis, several thermal parameters were defined and associated with the corresponding thermochemical processes: mass losses associated with water or hydroxyl formations, allotropic transformation, crystallizations, etc. (see Table 1).

Both intensity and temperature were systematically compared; results are presented in table form for better visualization. The local maximum or minimum was employed for temperature assignment, even though it is well known that in thermal analysis these do not have a thermodynamic meaning.

The thermal transformations processes of kaolinite (K) in kaolinitic clays is known to consist of a dehydroxylation into metakaolin (MK) at ≈ 600 °C, followed by the formation of a spinel type aluminosilicate (SAS) at ≈ 980 °C, and finally the development of mullite (M) at higher temperatures (1200–1300 °C) (Eq. 1- Eq. (5)).

Simultaneously, the dehydroxylation of each borate occurs. The processes and temperatures associated with the thermal program are shown in Table 1.

3.2. Thermogravimetric and differential thermal analysis (TG- DTA) of the boric acid-clay mixtures

Table 2 shows the temperature associated with the loss of mass of the clay (T) and clay-boron source mixtures obtained from the thermogravimetric curves. Fig. 1 shows the thermogravimetric curves of the studied mixtures (TG and dTG/dT), Fig. 2 shows the differential thermal analysis curves (DTA), and the pure clay is shown as well. The thermal parameters are presented in Table 2. The surface water loss is observed in all the mixtures, as well as in the non-added sample (endothermic peak), values are similar, and the slight difference might be explained by differences in the drying process.

Afterwards, the crystallization water losses of the boron sources are observed; in the synthetic borates studied (boric acid and borax) the loss of water of crystallization occurs between 25 and 500 °C, which coincides with the reference values [28,29].

In the case of natural borates, a greater number of thermal processes are observed due to their structural and mineralogical complexity. The temperature corresponding to dehydration for ulexite is between 45 and 150 °C and for colemanite between 350 and 400 °C.

After the dehydration of borates, the dehydration of kaolinite (K) takes place to obtain metakaolinite (MK) Eq. (1). The temperature associated with this process for (T) was 487 °C. With the addition of boric acid this was not affected, but yes with the rest of the additives; with the incorporation of borax it was 550 °C, while for colemanite and ulexite it was 558 and 550 °C respectively. This shows the influence of boron sources on the dehydration temperature. The presences of these oxides, lowers de fusion temperatures and affect the dehydroxilation mechanism.

The re-crystallization of natural borates is observed in marked exothermic processes around 700 °C; colemanite recrystallizes transforming into CaB_2O_4, while ulexite recrystallizes into CaB_2O_4 and NaB_3O_5 [28]. The re-crystallization process of colemanite was evidenced, showing a shoulder between 670 and 780 °C [28,29].

Regarding the DTA curves, the chemical processes of the boron sources were again corroborated and the advancement of the pre-mullite (spinel) formation peak was observed, at 980 °C [8,30] in all cases. This shows that the mechanism of formation of mullite is influenced by the presence of boron oxide (forming glass SiO_2 - B_2O_3). The maximum advancement observed was at 900 °C in the formula with ulexite as a sintering additive (T-U), then with borax (T-B) and finally with colemanite (T-C).

On the other hand, the signal in the DTA, corresponding to the formation of mullite (≈1200 °C), is not identified in the mixtures with the additives tested. Confirming again the interference in the mullite formation mechanism.

Finally, slight progressive mass loss is observed only in the mixtures above 1200 °C; this can be explained as a partial evaporation of boron oxides, which was previously observed in alumina boron systems.

3.3. Dilatometric analysis

The macroscopic thermal behavior of the clay and clay mixtures was recently fully described by Zanelli [10,31]. The present studied materials revealed a similar behavior. In Fig. 3 shows the dilatometric curves of the studied mixtures (TMA and dTMA/dT). In this, the first thermal expansion (positive slope in the TMA) range can be observed, from room temperature to 500 °C; this corresponds to the thermal expansion of the clay mineral. At 573 °C, the quartz transformation can be observed (a clear peak in the DTMA curves). This is not affected by the boron sources incorporation.

After this temperature, a flat zone is observable which finishes with a minor inflection stage at T 980 °C, where an abrupt 1% sigmoidal shrinkage can be observed in the TMA curve and a clear peak in the DTMA curve. These processes can be associated with the DTA spinel formation peak (Fig. 2). After the spinel formation, a slight shrinkage stage can be observed that finishes at 1080 °C; the 980 °C shrinkage, clearly observed in the pure clay, is slightly observed in the T-A and T-B; the T-C and T-U samples the contraction is advanced 50 °C. This peak (DTMA) corresponds to the SAS formation [30]; this flattens and moves into lower temperatures (down to 862 °C). The liquid boron oxide formed at lower temperatures (Fig. 3) strongly affects the transformation from metakaolinite to SAS. This thermal process consists in the formation of amorphous silica phase and the nanocrystalline spinel phase. The SiO_2–B_2O_3 binary system presents a low eutectic point slightly above 500 °C [32]. Hence, the eutectic formation enhances the MK into SAS transformation. This is verified by the temperature decrease in the corresponding DTMA peak, as shown in Fig. 3.

After these processes, the viscous sintering process occurs. This shrinkage consists in a three-step process for the pure clay (T). Three peaks can be devised in the DTMA curve, with easily definable peaks at 947 °C and 1173 °C and as a shoulder at 1230 °C [31]. This corresponds to the glassy viscous silica-based phase formed by the produced silica

Table 1
Processes and temperatures associated with the thermal program.

Associated process	Temperature (°C)
a Loss of surface water	40–100
b Dehydration of the oxidic source of boron	90–170
i. Boric acid	
ii. Borax	
iii. Colemanite	
iv. Ulexite	
c Allotropic transformation of quartz (α→β)	573
d. Kaolinite dehydration (K) $Al_2O_3.2SiO_2.2H_2O \rightarrow Al_2O_3.2SiO_2 + 2\,H_2O$	450–570
e Transformations of the oxidic source of boron	350 -600 [1]
f Formation of (SAS) and primary mullite (Mi) $Al_2O_3.2SiO_2(MK) \rightarrow spinel\ Al-Si\ (SAS)$ $Al_2O_3.2SiO_2(MK) \rightarrow 3Al_2O_3.2SiO_2(Mi)$	980
g Secondary mullite formation (Mii) $espinela\ Al-Si\ (SAS) + SiO_2(V) \rightarrow 3Al_2O_3.2SiO_2(Mii) + SiO_2(V)$	1200
h Boron loss $B_2O_{3(l)} \rightarrow B_2O_{3(g)}$	1250–1400

Table 2
Thermogravimetry, temperature associated with the loss of mass of the clay and clay-boron sources mixtures.

Process	Temp. (°C)	Mass loss (%)				
		T	T-Ac	T-B	T-C	T-U
a. Surface water loss	40–100	0.9	1.07	1.34	1.9	1.64
b. Dehydration of borates		–	3.3	1.46	1.32	1.26
c. Quartz allotropic transformation (α→β)	573					
d. Kaolinite dehydroxylation $Al_2O_3.2SiO_2.2H_2O\ (K) \rightarrow Al_2O_3.2SiO_2(MK) + 2\ H_2O$	450–570	6.46	6.0	6.25	6.05	5.78
e. Spinel and premullite formation $Al_2O_3.2SiO_2(MK) \rightarrow espinel\ Al-Si\ (SAS)$ $Al_2O_3.2SiO_2(MK) \rightarrow 3Al_2O_3.2SiO_2(Mi)$	980	–	–	–	–	–
f. Secondary mullite formation (Mii) $spinel\ Al-Si\ (SAS) + SiO_2(V) \rightarrow 3Al_2O_3.2SiO_2(Mii) + SiO_2(V)$	1200	–	–	–	–	–
g. Boron evaporation $B_2O_{3(l)} \rightarrow B_2O_{3(g)}$	1250–1400	–	1.66	0.34	0.31	0.12

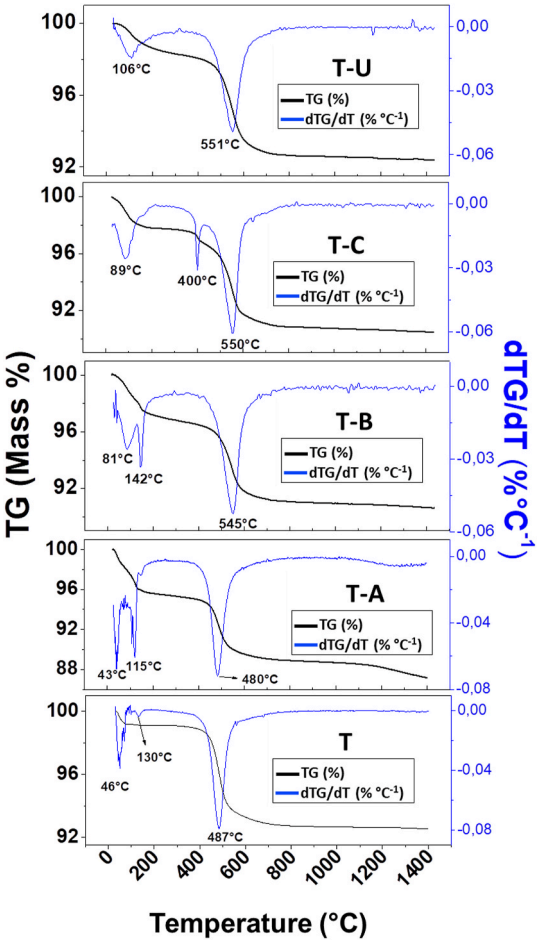

Fig. 1. Thermogravimetric curves of the Tincar clay (T) and clay– boron sources mixtures (T-A; T-B; T-C and T-U).

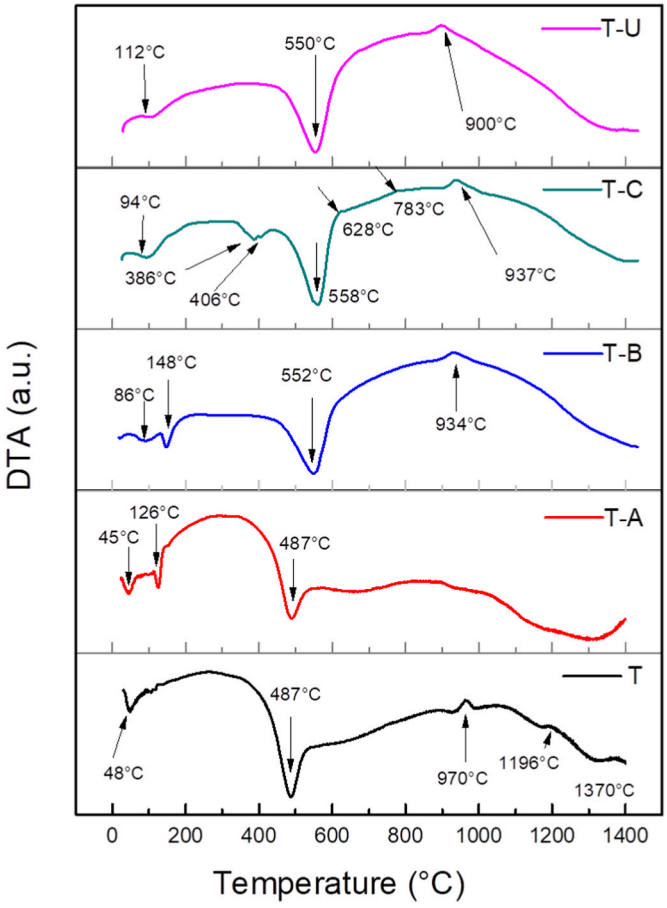

Fig. 2. Differential thermal analysis of the Tincar clay (T) and clay– boron sources mixtures (T-A; T-B; T-C and T-U).

originated in the clay decomposition. The mullite formation is observed at higher temperatures (above 1200 °C). The incorporation of boron oxide evidently affects these processes; in fact, the previously formed SiO_2–B_2O_3 (T-A) glassy phase lowered these reactions and processes. This low-viscosity phase enhances the sintering processes, and the alkali and earth alkali oxides dissolve into ternary and quaternary glass, which is responsible for the sintering. In this case, the amount of alkali is provided by the studied borates (borax: Na_2O, colemanite: CaO y ulexite: Na_2O and CaO). This phenomenon would also occur if feldspars or other alkali sources are added to the material formulation. During sintering, pores are collapsed, mullite phase is formed, and quartz is partially dissolved by the active multiphase silica-based glass [40] or irreversibly transformed into cristobalite [9]; the XRD analysis is shown below.

The mixture carried out with colemanite, presents a particular case, at 400 °C a negative peak is clearly seen, which corresponds to an expansion in the dilatometric curve, this process is also evidenced in thermogravimetry and differential thermal analysis, where it is observed the loss of water of constitution of this mineral at the mentioned temperature. When boron minerals are exposed to heat, the mineral first loses crystalline water, followed by the transformation of amorphous material or recrystallization into new phases [29,33]. The structure of

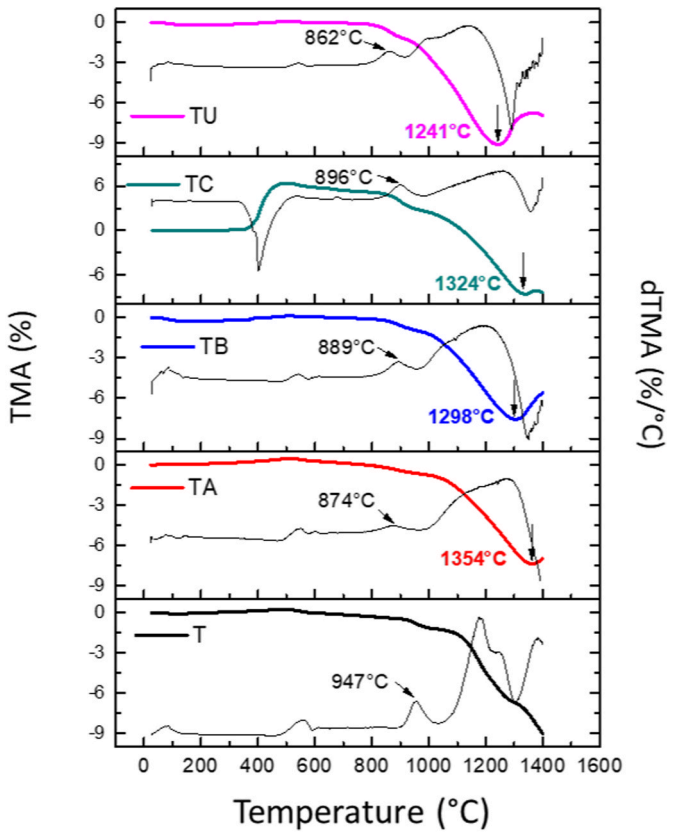

Fig. 3. TMA curves (dilatometry) of the Tincar clay (T) and clay– boron source mixtures (T-A; T-B; T-C; T-U). In all cases, the black curve represents the derivative of the TMA (DTMA).

colemanite involves water molecules locked within the structure and the rapid increase in internal pressure causes an explosive loss of water.

Sintering additives react with the other constituents of the mixtures during heating to form the glassy phases. The resulting glassy phase fills the porosity in the microstructure and leads to densification of the ceramic, which is evidenced by the minimum of the dilatometric curve.

The final sinterization temperature, assumed as the local minimum in the TMA curve, follows the T-U < T-B < T-C < T-A sequence. The pure fire clay sample does not reach the local minimum in the studied temperature range; the optimum (or maximum) sinterization would only be achieved at higher temperatures.

This analysis makes it possible to elucidate on the accessory oxides effect that accompany each boron source. The relative viscosity of the vitreous phase formed in case would have the following trend according to the values obtained from the TMA and dTMA/dT curves: the Na_2O and CaO combination given by ulexite is less than Na_2O contributed by borax, and this less than the CaO contributed by colemanite.

This fact also suggests the fluxing role of the studied additives. The completed shrinkage is almost constant for the four samples (≈7%). Above this temperature, an over-firing is observed for the three samples. This macroscopic enlargement is accompanied by the formation of gas bubbles, insoluble at this temperature [2,40].

3.4. Sintering parameters: open porosity (P) and apparent density (D)

Sintering advance is usually followed by Archimedes immersion test. Both open porosity (P) and apparent density (D) are determined from these tests. Porosity is strongly related to the mechanical behavior and thermal insulating properties of ceramics [43–46], which determine their actual technological applications.

The solely clay-based material porosity decreased from 24 to 14% between 1100 and 1400 °C sintering programs.

The obtained ceramics from binary mixtures present a clear tendency. In every case, the boron found addition resulted in lower porosities, in the 1200–1300 °C range; this can be clearly observed in Fig. 4, where the open porosity (P) is plotted as a function of the boron sources for the four temperatures studied. Boric acid can be understood as a fluxing agent. The porosity of materials is increasing in the following sense: B ≈ U <Ac <C <T (1200 °C); B <Ac <U <C <T (1300 °C).

In general, the trend is B <U <Ac <C; since the best degree of sintering is achieved with the minimum porosity, we can order the boron sources as follows according to their fluxing power B> U> A> C. Taking into account that borax is a sodium borate, ulexite is a sodium and calcium borate; and the colemanite of calcium; the fluxing power is attributed to the fact that the sodium oxide present in borax and ulexite makes the vitreous phase less viscous and achieves the best sintering, with porosity levels between 0.25 and 2.26% found in the suitable range for consideration as porcelain stoneware. With respect to boric acid, it presents an intermediate behavior and. Finally colemanite, which, by containing calcium oxide, makes the glassy phase more viscous, resulting in harder and more porous material.

Vitrification demonstrates a high level of fusion leading to almost zero (<3.0%) open porosity and a higher amount of glass phase (>40%) in the microstructure of ceramic materials (Iqbal and Lee 2000; Lee and Iqbal 2001; Martín-Márquez et al., 2009).

Among the different boron sources, the Na_2O/CaO ratio governs in terms of sinterability. The K_2O/MgO ratio remains approximately constant, since these oxides come clearly from clay, we then see that the Na_2O/CaO ratio governs, with Na_2O being the most active as a flux, which is consistent with the data obtained on the order of flux character of boron sources: B> U> Ac> C.

The achieved apparent density is within the expected values (Fig. 4) [2]. The pure mineral-based materials (T) fall between 1.95 and 2.08 g cm^{-3}. As expected, higher densities are obtained after higher temperature programs.

3.5. Developed crystalline and non-crystalline phases proportions of the developed ceramics fired at 1200 and 1300 °C by the Rietveld method and the Le Bail approach

The diffraction patterns show the presence of both crystalline and non-crystalline glassy phases. The identified crystalline phases and employed crystallographic cards are shown in Table 3. The typical silica-based amorphous band can be easily observed in the boron-containing samples. The crystalline phases identified and quantified for the six samples were mullite ($3Al_2O_3{\cdot}2SiO_2$), cristobalite (SiO_2) and quartz (SiO_2).

The shape of the cristobalite peaks could not be satisfactorily fitted by a single contribution. Two different cristobalite structures were proposed for the Rietveld refinement. This was previously proposed for similar materials [34–36]. Refined cell parameters for both cristobalites are shown in Table 3. This might be explained by the coexistence of two dissimilar phases, with different presence of impurities: one produced from the kaolinite thermal decomposition and the other from the thermal transformation of the initial quartz present in the clay mineral, the second one presenting lower impurities content.

It is well known that the AI_2O_3– SiO_2–Re_2O_3 systems (Re: metal) are characterized by their glass-forming abilities [8, 37–39] and the boron element is a metalloid; in this case, the behavior is similar to metals. Boron is a glass former element [18]. It is worth remembering that the binary SiO_2–B_2O_3 phase system presents a eutectic temperature of approximately 500 °C.

Fig. 5 shows the quantification of each phase for the obtained materials at 1200 and 1300 °C. It can be observed for the set of materials obtained from Tincar clay at 1200 °C, that the addition of boron sources produces an increase in the glass phase at the expense of the decrease in

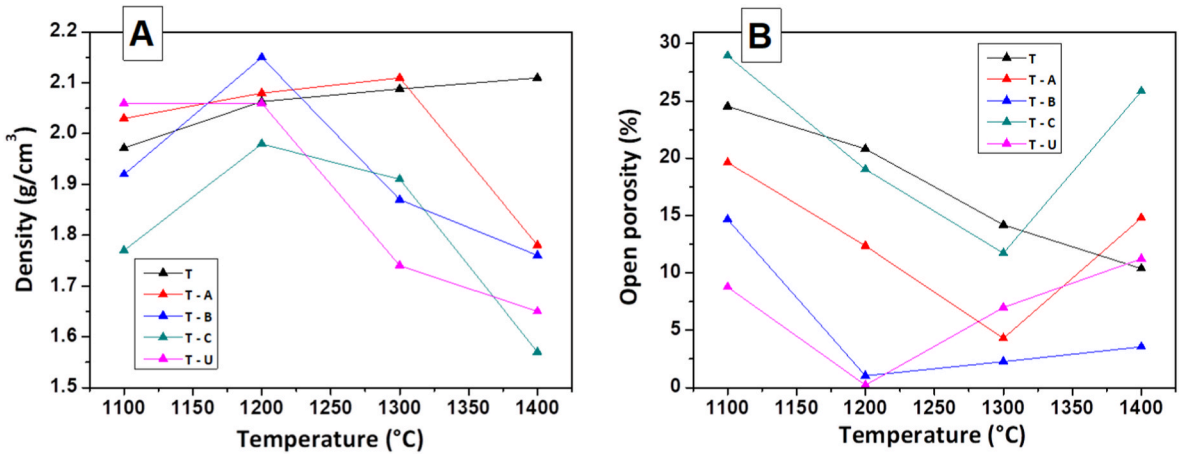

Fig. 4. A- Apparent densities of the studied materials, effect of the initial composition and firing temperature. B- Open porosity of the studied materials, effect of the initial composition and firing temperature.

Table 3
Identified crystalline phases, chemical formula and employed PDF card.

Crystalline phases	Formula	PDF card or method
Quartz	SiO_2	01-079-1910
Mullite	$3Al_2O_3{\cdot}2SiO_2$	01-079-1275
Cristobalite	SiO_2	01-082-0512
Cristobalite 2	SiO_2	01-082-0512
Glassy phase Silica	SiO_2	Le Bail approach [29, 47]

quartz, fundamentally, although a slight decrease in mullite is observed, in comparison to the material without additives (T −1200).

Of the four boron sources studied, the ones with the least glassy phase in the ceramic material are boric acid and colemanite.

At 1300 °C the ceramic T −1300 shows a noticeable increase in the cristobalite phase, at the expense of quartz and the glass phase; mullite remains practically constant when passing from 1200 to 1300 °C. With regard to the influence of boron sources at this temperature, an increase in the glass phase is observed in the four ceramic materials (T-Ac 1300; T-B 1300; T-C 1300; T-U 1300). Colemanite is the source of boron that generates the least vitreous phase, on the other hand, quartz and cristobalite remain in its final composition.

Regarding boron sources in ceramic material, a similar trend is observed between borax and ulexite, colemanite has a behavior similar to boric acid at 1200 °C.

Fig. 5 presents the phase composition evaluated by the Rietveld method. Global estimated standard deviations were below 2 mass %. In all cases, they were derived from the estimated standard deviation on individual scale factors, for the respective phases. The goodness of the Rietveld refinement is usually represented by the Rwp parameter. The Rwp values are adequate (Rwp ≤15 in all the cases) and similar to the ones achieved in similar materials [40,41]. No boron-containing crystalline phases were detected.

3.6. *Pore size distribution by mercury intrusion porosimetry of the ceramics fired at 1300 °C*

In order to observe and compare the microstructural differences of the materials elaborated with the different boron source under equivalent processing conditions, a comparative study of mercury intrusion porosimetry was carried out. The pore distribution and size would show possible differences in the sintering mechanisms or in the degree of

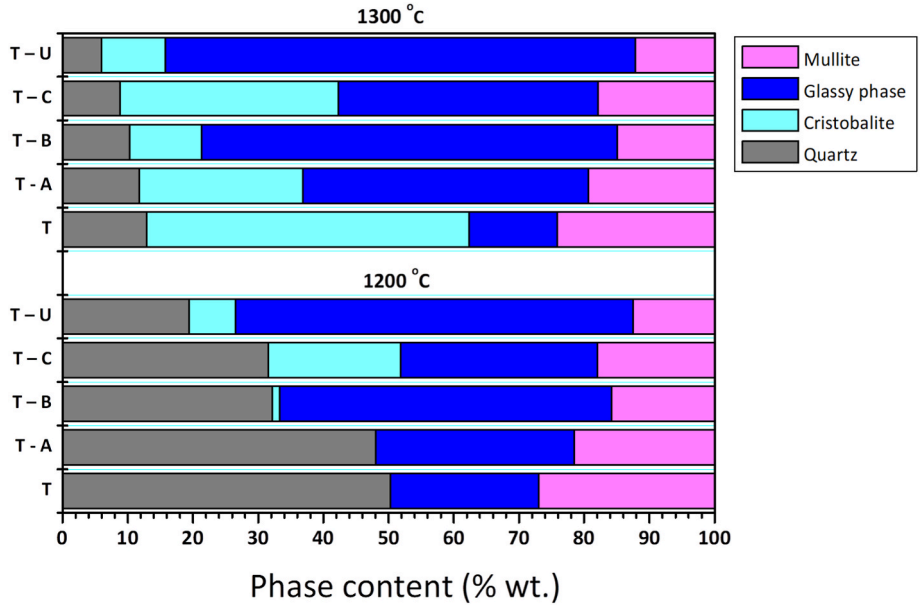

Fig. 5. Crystalline and glassy phase content as a function of boron source addition, after firing (1200 and 1300 °C).

sintering (or de-sintering) of materials.

Fig. 6 shows the pore size distributions of the materials obtained from Tincar clay with the four boron sources at 1300 °C. In all cases there is evidence of a decrease in the average pore size of the materials with the addition of sintering additives.

The sintering additives managed to reduce the average pore size (d50) with respect to the T - 1300 material. The sequence was as follows: T (≈550 nm)> T-C (≈310 nm)> T-B (≈140 nm)> T-U (≈98 nm)> T-A (≈80 nm), the same sequence is reproduced at the smallest pore sizes (d90).

The larger pore sizes, represented with the d10, turned out to be smaller than the material T −1300, with the exception of the TC which presented a d90 of 3570 nm and a bimodal pore size distribution; these facts show the lower degree of sintering (presence of macropores) of T - C.

3.7. Microstructure analysis developed in ceramics fired a 1300 °C by scanning electron microscope

The developed microstructures, after firing the clay and clay–boric acid mixtures at 1300 °C, were evaluated by means of scanning electron microscopy; the relatively dense and complex microstructure of the ceramics is revealed (Fig. 7). In images with lower magnification (×500 images: a, d, g, j and m), pores (in black) can be identified in the matrix (different shades of gray). Chemical etching was carried out in the x 1000 and x 2000 micrographs (b, c, e, f, h, I, k, l, n and ñ), and this permits us to observe the crystalline grains.

The matrix can be described as a complex microstructure of crystalline grains (several microns) embedded in the glassy (amorphous–viscous) continuous phase. Grains correspond to the crystalline phases detected by XRD: mullite, quartz and cristobalite. The glassy phase, predominantly silica based, was also observed. Porosity correlates with the boron source addition and follows the sequence T-B < T-Ac < T-U < T-C <T, as evaluated by the Archimedes method (Fig. 4). Rounded macro-pores (≈100 μm) are complemented by a micro (meso)-porosity only observed in greater magnifications. The observed microstructures are equivalent to those extensively reported in the literature [19,22,42].

Fig. 7 shows the images obtained by SEM corresponding to the ceramics obtained from Tincar clay and the different boron sources, sintered at 1300 °C. In the four materials, a clear porosity between approximately 50 and 100 μm can be observed. That corresponding to the material with ulexite (T-U) is a surface porosity, relatively uniform

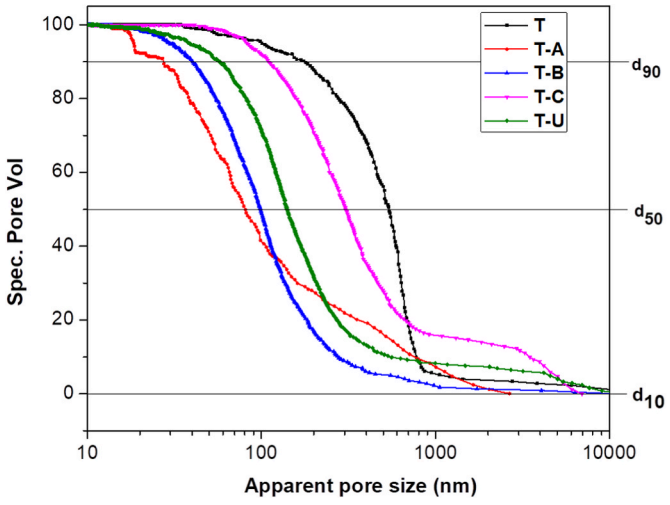

Fig. 6. Open pore size distribution of the ceramics based in Tincar clay (T) and clay– boron source mixtures (T-A; T-B; T-C; T-U) by mercury intrusion porosimetry.

and not connected with the interior of the ceramic; the opposite occurs with materials developed with boric acid (T-A), borax (T-B) and colemanite (T-C), this is better visualized in the images with lower magnification, giving a general perspective of the materials. As the magnification increases, the phases already identified by X-ray diffraction begin to become evident, which are: quartz (Q), mullite (M), cristobalite (C) and glass phase (V). As the magnification increases, the pore size distribution becomes noticeable, although it remains in the aforementioned range, and comparable with the porosimetry results (see Fig. 6).

As the magnification increases, quartz, primary and secondary mullite, and cristobalite inlays begin to be seen. The formation of secondary mullite is evident in the materials T-A 1300 and T-B 1300, in the material T-C 1300, no secondary mullite is identified, which has to do with the lower formation of the glass phase of the three materials discussed in this section, and remembering that secondary mullite (needle-shaped) crystallizes from the glassy phase rich in alumina around 1200 °C, and the T-U material presents an intermediate situation between these.

As explained in the previous section, through the quantification of the phases present in the materials by the Rietveld method, the amount of mullite is independent of the source of boron used; here a difference is made between the primary mullite and the secondary one, which come from different forming mechanisms.

It can be seen that the mullite needles for the materials T-A 1300 and T-B 1300 have an approximate aspect ratio of length: width of approximately 20: 1, while in the other materials it is difficult to visualize this relationship. It is observed that they are smaller in diameter and length.

4. Conclusions

The effects of different boron sources on the thermal behavior, the textural properties, the microstructure and the mineralogical composition, in ceramic materials based on a kaolinitic clay, were studied.

The thermal behavior of the mixtures was described. With respect to the exothermic peak (970 °C) corresponding to the formation of pre-mullite (SAS) it was affected, in comparison to the clay without additives.

The pure clay (T) did not present a minimum in the dilatometric curve in the studied temperature range. Using the flux agents a minimum was observed, evidencing an expansion process.

Of the boron sources used, those that showed the best fluxing effect were borax and ulexite, reaching almost zero porosity and maximum density in the optimal sintering range, which was between 1200 and 1300 °C.

It is evident that the sodium oxide content in borax and ulexite decreases the viscosity of the formed glass around 1000–1050 °C. That is the reason for the early appearance of the SAS peak.

The resulting phases were identified and quantified after the thermal treatments at 1200 and 1300 °C by the Rietveld method, including the amorphous phase with the Le Bail approach. The mullitization degree was consistent with the initial amount of kaolinite in the clay.

The materials microstructure, after the 1300 °C heat treatment, showed quartz, cristobalite, mullite, and a glassy phase, as it was also identified by XRD. Secondary mullites showed different width: length aspect ratios and this is related to the different viscosity of the glassy phase where they come from. The presence of calcium makes the vitreous phase more viscous which results in rod-like rather than needle-like morphologies.

The additives containing sodium oxide are responsible for the lower viscosity favoring the formation of the secondary mullite (Mii).

The performed study contributes to establish criteria and strategies for the design of ceramic formulations with direct incorporation of boron sources.

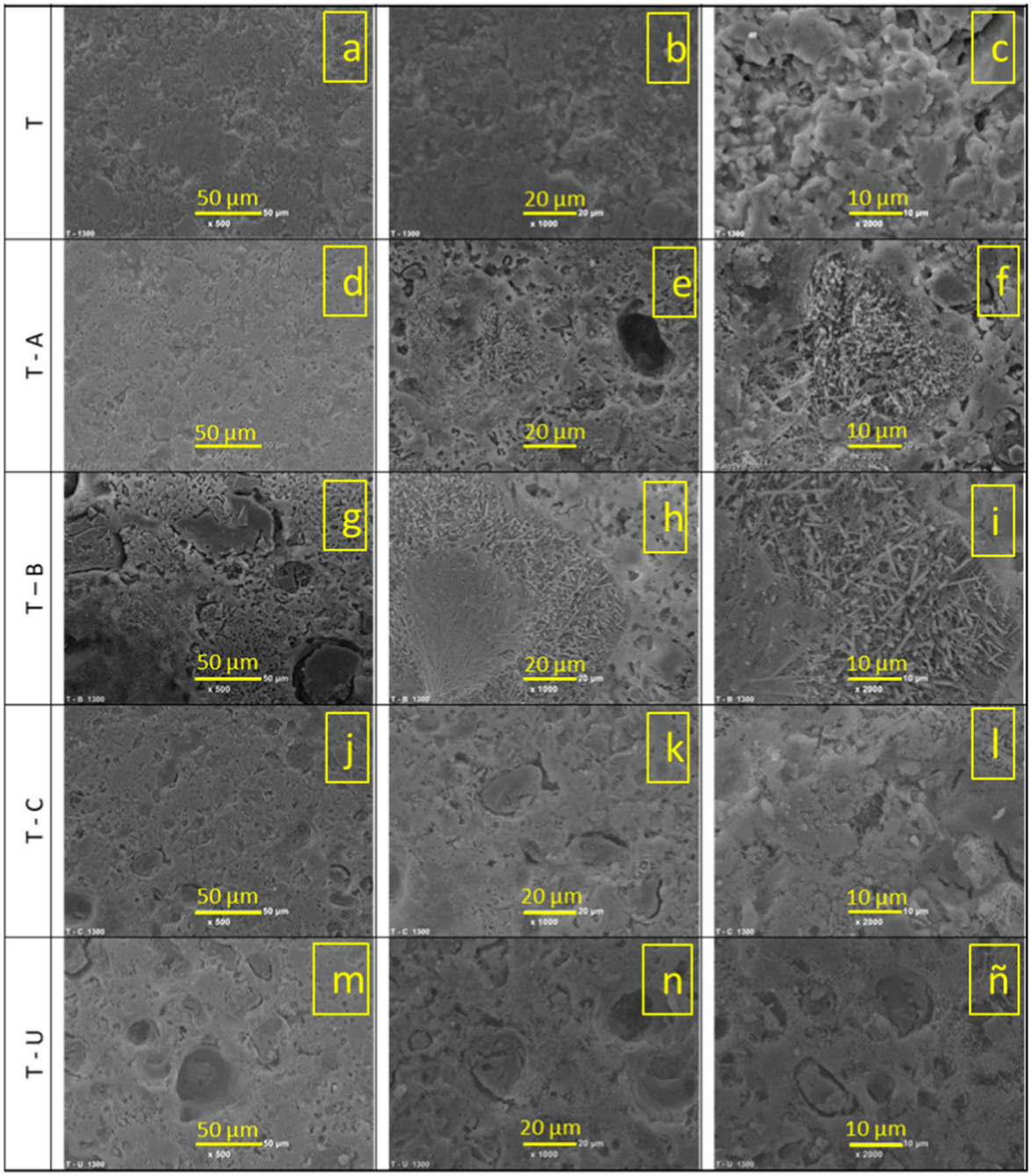

Fig. 7. SEM images of the clay and clay – boron sources mixtures fired at 1300 °C (T: a–c; T-A: d–f; T-B: g–i; T-C: j–l; T-U: m–ñ) respectively (from left to right: 500×, 1000× and 2000×).

Declaration of competing interest

The authors declare that they have no known competing financial interests or personal relationships that could have appeared to influence the work reported in this paper.

Acknowledgments

This work has been supported by the Argentinian funding institutions Consejo Nacional de Investigaciones Científicas y Técnicas (CONICET), Agencia Nacional de Promoción Científica y Tecnológica ' (ANPCyT, PICT 2016-1193), and Universidad Nacional de La Plata (UNLP, X-904). PVL CONICET for the scholarship. Finally, MFH and NMR are members of CONICET, Argentina.

References

[1] C.F. Revelo, H.A. Colorado, 3D printing of kaolinite clay ceramics using the Direct Ink Writing (DIW) technique, Ceram. Int. 44 (2018) 5673–5682, https://doi.org/10.1016/j.ceramint.2017.12.219.

[2] S. Chen, W.-H. Cai, J.-M. Wu, Y.-X. Ma, C.-H. Li, Y.-S. Shi, C.-Z. Yan, Y.-J. Wang, H.-X. Zhang, Porous mullite ceramics with a fully closed-cell structure fabricated by direct coagulation casting using fly ash hollow spheres/kaolin suspension, Ceram. Int. 46 (2020) 17508–17513, https://doi.org/10.1016/j.ceramint.2020.04.046.

[3] D. Redaoui, F. Sahnoune, M. Heraiz, N. Saheb, Phase formation and crystallization kinetics in cordierite ceramics prepared from kaolinite and magnesia, Ceram. Int. 44 (2018) 3649–3657, https://doi.org/10.1016/j.ceramint.2017.11.119.

[4] F.G. Melchiades, L.R. Dos Santos, N. Suelen, A.O. Boschi, Agentes fundentes para las piezas de gres porcelánico producidas por vía seca, in: Congreso Mundial de La Calidad Del Azulejo y Del Pavimento Cerámico, QUALICER), 2012, pp. 1–12.

[5] E.N. Lysenko, V.A. Vlasov, A.V. Malyshev, E.A. Sheveleva, A.P. Surzhikov, Microstructure and electromagnetic properties of LiFe5O8 ferrite ceramics

prepared from wet- and dry-milled powders, Ceram. Int. 47 (2021) 23935–23941, https://doi.org/10.1016/j.ceramint.2021.05.102.
[6] C. Detellier, Functional kaolinite, Chem. Rec. 18 (2018) 868–877, https://doi.org/10.1002/tcr.201700072.
[7] P.J. Sánchez-Soto, D. Eliche-Quesada, S. Martínez-Martínez, E. Garzón-Garzón, L. Pérez-Villarejo, J.Ma Rincón, The effect of vitreous phase on mullite and mullite-based ceramic composites from kaolin wastes as by-products of mining, sericite clays and kaolinite, Mater. Lett. 223 (2018) 154–158, https://doi.org/10.1016/j.matlet.2018.04.037.
[8] L. Andrini, M.R. Gauna, M.S. Conconi, G. Suarez, F.G. Requejo, E.F. Aglietti, N. M. Rendtorff, Extended and local structural description of a kaolinitic clay, its fired ceramics and intermediates: an XRD and XANES analysis, Appl. Clay Sci. 124–125 (2016) 39–45, https://doi.org/10.1016/j.clay.2016.01.049.
[9] F.G. Melchiades, AGENTES FUNDENTES PARA LAS PIEZAS DE GRES PORCELÁNICO PRODUCIDAS POR VÍA SECA, (n.d.) 12.
[10] C. Zanelli, M. Raimondo, G. Guarini, M. Dondi, The vitreous phase of porcelain stoneware: composition, evolution during sintering and physical properties, J. Non-Cryst. Solids 357 (2011) 3251–3260, https://doi.org/10.1016/j.jnoncrysol.2011.05.020.
[11] E. Sánchez, J. García-Ten, V. Sanz, A. Moreno, Porcelain tile: almost 30 years of steady scientific-technological evolution, Ceram. Int. 36 (2010) 831–845, https://doi.org/10.1016/j.ceramint.2009.11.016.
[12] M. Dondi, M. Raimondo, C. Zanelli, Clays and bodies for ceramic tiles: reappraisal and technological classification, Appl. Clay Sci. 96 (2014) 91–109, https://doi.org/10.1016/j.clay.2014.01.013.
[13] F.G. Melchiades, M.T. Daros, A.O. Boschi, Porcelain tiles by the dry route, Bol. Soc. Espanola Ceram. Vidr. 49 (2010) 221–226.
[14] F.G. Melchiades, L.R. dos Santos, S. Nastri, A.O. Boschi, Alternatives in the body composition of porcelain tiles produced by the dry route, Cfi-Ceram. Forum Int. 89 (2012) E39.
[15] G.N. Angelopoulos, A. Christogerou, T. Kavas, Y. Pontikes, S. Koyas, Y. Tabak, Boron Waste as a Flux in the Heavy Clay Industry, 2008.
[16] M.A.L. Braulio, G.G. Morbioli, V.C. Pandolfelli, Advanced boron-containing Al2O3-MgO refractory castables, J. Am. Ceram. Soc. 94 (2011) 3467–3472, https://doi.org/10.1111/j.1551-2916.2011.04608.x.
[17] A.P. Luz, J.H. Gagliarde, C.G. Aneziris, V.C. Pandolfelli, B4C mineralizing role for mullite generation in Al2O3-SiO2 refractory castables, Ceram. Int. 43 (2017) 12167–12178, https://doi.org/10.1016/j.ceramint.2017.06.075.
[18] I.D. Giovannelli Maizo, A.P. Luz, C. Pagliosa, V.C. Pandolfelli, Boron sources as sintering additives for alumina-based refractory castables, Ceram. Int. 43 (2017) 10207–10216, https://doi.org/10.1016/j.ceramint.2017.05.047.
[19] S. Kurama, A. Kara, H. Kurama, The effect of boron waste in phase and microstructural development of a terracotta body during firing, J. Eur. Ceram. Soc. 26 (2006) 755–760, https://doi.org/10.1016/j.jeurceramsoc.2005.07.039.
[20] T. Kavas, A. Christogerou, Y. Pontikes, G.N. Angelopoulos, Valorisation of different types of boron-containing wastes for the production of lightweight aggregates, J. Hazard Mater. 185 (2011) 1381–1389, https://doi.org/10.1016/j.jhazmat.2010.10.059.
[21] H.S. Soykan, Low-temperature fabrication of steatite ceramics with boron oxide addition, Ceram. Int. 33 (2007) 911–914, https://doi.org/10.1016/j.ceramint.2006.02.001.
[22] M.F. Hernández, M.A. Violini, M.F. Serra, M.S. Conconi, G. Suarez, N.M. Rendtorff, Boric acid (H3BO3) as flux agent of clay-based ceramics, B2O3 effect in clay thermal behavior and resultant ceramics properties, J. Therm. Anal. Calorim. 139 (2020) 1717–1729, https://doi.org/10.1007/s10973-019-08563-4.
[23] M.F. Cravero, E.A. Dominguez, Kaolin deposits in the lower cretaceous baqueró formation (Santa Cruz Province, Patagonia, Argentina), J. S. Am. Earth Sci. 6 (1992) 223–235, https://doi.org/10.1016/0895-9811(92)90043-X.
[24] D.L. Bish, J.E. Post, Quantitative mineralogical analysis using the Rietveld full-pattern fitting method, Am. Mineral. 78 (1993) 932–940.
[25] D.L. Bish, S.A. Howard, Quantitative phase analysis using the Rietveld method, J. Appl. Crystallogr. 21 (1988) 86–91, https://doi.org/10.1107/S0021889887009415.
[26] A. Le Bail, Modelling the silica glass structure by the Rietveld method, J. Non-Cryst. Solids 183 (1995) 39–42, https://doi.org/10.1016/0022-3093(94)00664-4.
[27] Quantitative analysis of silicate glass in ceramic materials by the Rietveld method (n.d.), http://www.ing.unitn.it/~luttero/Publications/EPDIC_V/silicate_glass.html. (Accessed 16 February 2018).
[28] F. Gazulla, M.P. Gómez Tena, M. Orduña, G. Silva, Chemical, Mineralogical and Thermal Characterisation of Natural and Synthetic Boratesales, 2005.
[29] S. Akpinar, A. Evcin, Y. Ozdemir, Effect of calcined colemanite additions on properties of hard porcelain body, Ceram. Int. 43 (2017) 8364–8371, https://doi.org/10.1016/j.ceramint.2017.03.178.
[30] K. Okada, N. Otsuka, J. Ossaka, Characterization of spinel phase formed in the kaolin-mullite thermal sequence, J. Am. Ceram. Soc. 69 (1986), https://doi.org/10.1111/j.1151-2916.1986.tb07353.x. C-251-C–253.
[31] M. Dondi, C. Iglesias, E. Dominguez, G. Guarini, M. Raimondo, The effect of kaolin properties on their behaviour in ceramic processing as illustrated by a range of kaolins from the Santa Cruz and Chubut Provinces, Patagonia (Argentina), Appl. Clay Sci. 40 (2008) 143–158, https://doi.org/10.1016/j.clay.2007.07.003.
[32] S.A. Decterov, V. Swamy, I.-H. Jung, Thermodynamic modeling of the B2O3-SiO2 and B2O3-Al2O3 systems, Int. J. Mater. Res. 98 (2007) 987–994, https://doi.org/10.3139/146.101555.
[33] C. Eymir, H. Okur, Dehydration of ulexite by microwave heating, Thermochim. Acta 428 (2005) 125–129, https://doi.org/10.1016/j.tca.2004.11.003.
[34] M.A. Butler, D.J. Dyson, The quantification of different forms of cristobalite in devitrified alumino-silicate ceramic fibres, J. Appl. Crystallogr. 30 (1997) 467–475, https://doi.org/10.1107/S0021889897001672.
[35] I.C. Madsen, R.J. Finney, R.C.A. Flann, M.T. Frost, B.W. Wilson, Quantitative analysis of high-alumina refractories using X-ray powder diffraction data and the Rietveld method, J. Am. Ceram. Soc. 74 (1991) 619–624, https://doi.org/10.1111/j.1151-2916.1991.tb04069.x.
[36] M.F. Hernández, M.S. Conconi, M. Cipollone, M.S. Herrera, N.M. Rendtorff, Ceramic behavior of ball clay with gadolinium oxide (Gd2O3) addition, Appl. Clay Sci. 146 (2017) 380–387, https://doi.org/10.1016/j.clay.2017.06.021.
[37] M.F. Serra, M.S. Conconi, G. Suarez, E.F. Agietti, N.M. Rendtorff, Firing transformations of an argentinean calcareous commercial clay, Cerâmica 59 (2013) 254–261, https://doi.org/10.1590/S0366-69132013000200010.
[38] M.S. Conconi, M.R. Gauna, M.F. Serra, G. Suarez, E.F. Aglietti, N.M. Rendtorff, Quantitative firing transformations of a triaxial ceramic by X-ray diffraction methods, Cerâmica 60 (2014) 524–531, https://doi.org/10.1590/S0366-69132014000400010.
[39] U. Kolitsch, H.J. Seifert, F. Aldinger, Phase relationships in the system Gd2O3-Al2O3-SiO2, J. Alloys Compd. 257 (1997) 104–114, https://doi.org/10.1016/S0925-8388(96)03121-0.
[40] R.D. Bonetto, P.E. Zalba, M.S. Conconi, M. Manassero, The Rietveld method applied to quantitative phase analysis of minerals containing disordered structures, Rev. Geol. Chile 30 (2003) 103–115.
[41] S. Hillier, Accurate quantitative analysis of clay and other minerals in sandstones by XRD: comparison of a Rietveld and a reference intensity ratio (RIR) method and the importance of sample preparation, Clay Miner. 35 (2000) 291–302.
[42] C. Zanelli, E. Domínguez, C. Iglesias, S. Conte, C. Molinari, R. Soldati, G. Guarini, M. Dondi, Recycling of residual boron muds into ceramic tiles, Bol. Soc. Espanola Ceram. Vidr. 58 (2019) 199–210, https://doi.org/10.1016/j.bsecv.2019.01.002.